

LVMark: Robust Watermark for latent video diffusion models

MinHyuk Jang^{1*} Youngdong Jang^{1*} JaeHyeok Lee¹ Kodai Kawamura¹ Feng Yang² Sangpil Kim^{1†}

¹ Korea University ² Google DeepMind

Abstract

Rapid advancements in generative models have made it possible to create hyper-realistic videos. As their applicability increases, their unauthorized use has raised significant concerns, leading to the growing demand for techniques to protect the ownership of the generative model itself. While existing watermarking methods effectively embed watermarks into image-generative models, they fail to account for temporal information, resulting in poor performance when applied to video-generative models. To address this issue, we introduce a novel watermarking method called LVMark, which embeds watermarks into video diffusion models. A key component of LVMark is a selective weight modulation strategy that efficiently embeds watermark messages into the video diffusion model while preserving the quality of the generated videos. To accurately decode messages in the presence of malicious attacks, we design a watermark decoder that leverages spatio-temporal information in the 3D wavelet domain through a cross-attention module. To the best of our knowledge, our approach is the first to highlight the potential of video-generative model watermarking as a valuable tool for enhancing the effectiveness of ownership protection in video-generative models.

1. Introduction

Video generative models have significantly enhanced their ability to create high-quality videos [3, 6, 24, 44, 54]. As these advancements increase the utility of video diffusion models, it is necessary to address the issue of model ownership infringement [12, 18, 41]. Since existing video watermarking methods embed the watermark into the video rather than the generative model [23, 39], they require costly post-processing for each video and cannot verify ownership if the generative model is stolen. As a way to establish ownership of generative models, embedding watermarks directly into diffusion models has recently collected

*Equal Contribution

†Corresponding Author

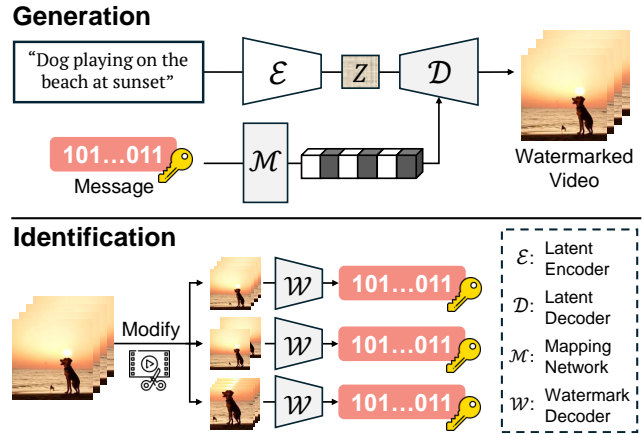


Figure 1. **Overview of video generation and ownership identification.** **Top:** A binary message is embedded in the latent decoder to generate a watermarked video. **Bottom:** The watermark decoder extracts message from modified videos (e.g., H.264 compression, frame drops, cropping) to identify the model ownership.

much attention [12, 18]. Inspired by watermarking methods for image diffusion models, in this paper, we propose a method to embed watermarks into video diffusion models to establish model ownership.

To the best of our knowledge, there does not exist a watermarking method for watermarks into video-generative models, but several approaches that embed watermarks into image diffusion models have been proposed so far [12, 42]. The key challenge is how to embed a watermark with minimal degradation of generated images. The common idea is to fine-tune the latent decoder of the image generator using loss functions focused on image quality and watermark accuracy; for example, Stable Signature [12] employ LPIPS [52] to assess watermarked image quality and binary cross-entropy loss for the watermark message.

In the absence of watermarking methods for video diffusion models, applying the watermarking methods from image to video diffusion models is essential. However, watermarking methods for image diffusion models do not consider video-specific features, such as temporal consistency and robustness to video-specific attacks. When image diffusion models [29, 32, 34] are applied to video dif-

fusion models, they fine-tune image-generative models to embed messages into each video frame using a 2D watermark decoder, which results in message embedding without considering inter-frame relationships. Moreover, these methods are vulnerable to video-specific attacks, such as H.264 compression, which is the widely used compression technology that easily removes messages embedded in the videos [8, 20, 23, 37, 43]. As these methods are trained to embed a single message into the model, they require a separate training process for each watermark message. Therefore, simply applying watermarking methods developed for image diffusion models is insufficient for video diffusion models.

To address these challenges, we introduce LVMark, a novel watermarking method specifically designed for video diffusion models. The goal of LVMark is to embed random binary messages into each frame of a video, enabling the generation of videos with different watermark messages after a single training process. To embed messages effectively while preserving video quality, we selectively modulate weight parameters in the latent decoder with minimal visual impact, enabling direct embedding of multiple random messages with single training [48]. Additionally, we design a robust watermark decoder that integrates the 3D wavelet domain which has spatio-temporal information with the RGB domain through a cross-attention module, which is shown to have the ability to effectively fuse two domains [15, 16]. To balance the trade-off between visual quality and message decoding accuracy, which is common in watermarking tasks, we propose a weighted patch loss that places more emphasis on patch areas where artifacts occur. Experimental results demonstrate that our method outperforms all the reasonable baselines. Since our method does not alter the structure of the diffusion model, it prevents anonymous users from bypassing the watermarking process. With its ability to identify AI-generated videos and verify ownership, LVMark protects ownership of the creations. Our contributions in this paper can be summarized as follows:

- We propose a novel watermarking method that embeds watermarks into video diffusion models, to the best of our knowledge, for the first time.
- By leveraging an importance-based weight modulation technique, our method embeds multiple messages into video diffusion models with a single training process while preserving video quality.
- Our watermark decoder is constructed to efficiently leverage the 3D wavelet domain, capturing the spatio-temporal information necessary for robust message decoding against video-specific attacks, including H.264 compression and frame drops.
- To balance visual quality with message decoding accuracy, we introduce a weighted patch loss that effectively

reduces artifacts in localized areas.

2. Related Work

2.1. Video Diffusion Models

Diffusion models have become a powerful generative approach, refining noisy data progressively to produce high-quality outputs [14, 27, 34, 36, 46]. Latent Video Diffusion Models (LVDMs) [4] optimize spatio-temporal features within a compact latent space, reducing computational costs. OpenSora [54] and Latte [24] utilize the DiT to model long-range temporal dependencies [28]. In contrast, Stable video diffusion [3] and VideoCrafter [6] leverage U-Net to effectively capture both spatial and temporal dependencies. DynamiCrafter [44] enhances U-net based methods by modeling dynamic scenes and complex motion [50]. Both U-Net and DiT architectures play crucial roles in advancing video generation, highlighting the need for watermark methods that can be applied to both types of video diffusion models.

2.2. 3D Discrete Wavelet Transform

3D discrete wavelet transform (3D DWT) is a classical method widely used to analyze temporal information of videos. 3D DWT operates along the time, height, and width of videos to decompose a low frequency subband and several high frequency subbands: LLL , LLH , LHL , LHH , HLL , HLH , HHL , and HHH each with a size of $F/2 \times H/2 \times W/2$, where L and H denote low and high frequency, while F , H , and W are frame, height, and width of video respectively. This operation analyzes the spatio-temporal information of videos. Existing video processing methods [11, 26, 47, 49, 51] utilize this property of 3D DWT to detect temporal information. Video digital watermarking methods [2, 17, 21, 22, 35] applied 3D DWT to the video for robustness of watermark. To the best of our knowledge, no research has yet explored watermarking video diffusion models using 3D DWT, underscoring the need for investigation to enhance robustness against common video modifications.

2.3. Diffusion Model Watermark

Digital watermarking plays a crucial role in protecting intellectual property, ensuring content authenticity, and enabling ownership tracking. Recently, digital watermarking technology has been applied to diffusion models. Watermarking methods for diffusion models [42, 45, 53] embed watermarks into the generated content from diffusion models without a post-processing step. However, since they mainly focus on the image-generative models, these methods perform poorly when applied to video diffusion models (Section 5.4), which highlights the need for research on watermarking in video-generative models.

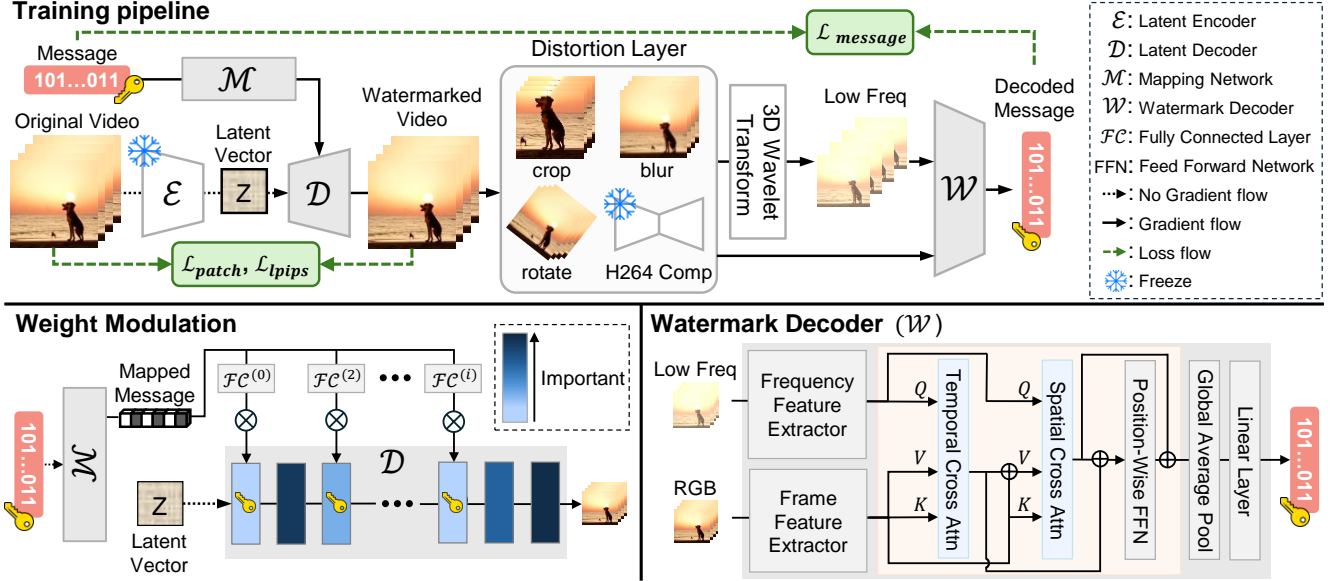


Figure 2. **Training Pipeline.** The training pipeline of our method is illustrated here. **Top:** We fine-tune the latent decoder to embed binary messages in generated videos and train the watermark decoder to retrieve messages from distorted videos. **Bottom-left:** We modulate layers of the latent decoder that minimally impact visual quality to embed random messages. **Bottom-right:** The watermark decoder combines the RGB video with low frequency subbands from a 3D wavelet transform using cross-attention to decode the binary message.

3. Preliminaries

We utilize latent video diffusion models, which consist of a latent encoder \mathcal{E} , a latent decoder \mathcal{D} , and a diffusion model, which is typically based on one of two architectures: U-Net [33] or DiT [28]. The latent encoder $\mathcal{E}(v)$ maps the video $v \in \mathbb{R}^{d_v}$ to a latent representation $z \in \mathbb{R}^{d_z}$, where d_v and d_z denote the dimensions of video v and latent vector z . In the forward process, noise is added to z , resulting in z_t , which is then denoised in the backward process to recover z , conditioned on inputs (e.g., text prompts). Finally, the latent decoder \mathcal{D} converts z back to the video $\hat{v} = \mathcal{D}(z)$. U-Net-based diffusion models focus on local features through downsampling and upsampling layers. In contrast, DiT-based models capture global dependencies and long-range correlations, making them effective for modeling complex temporal relationships. While image diffusion model watermarking methods [12, 31, 41] target U-Net-based models, we introduce a novel watermarking method applicable to both U-Net and DiT-based video diffusion models.

4. Methods

An overview of our method is shown in Figure 2. Our method fine-tunes the latent decoder \mathcal{D} to generate video frames while embedding invisible binary messages into each frame.

4.1. Importance-based Weight Modulation

Our method aims to embed random messages into video diffusion models, enabling the generation of videos with dif-

ferent watermark messages. To achieve this, inspired by Yu et al. [48], we modulate the weight parameters of pre-trained latent decoder \mathcal{D} based on importance of layers, as shown in bottom-left of Figure 2. For every iteration, we first transform the random message m into the mapped message m' with the mapping network $\mathcal{M}(m) : \mathbb{R}^{d_m} \rightarrow \mathbb{R}^{d_{m'}}$, which is composed of two fully connected layers. Then, we modulate the i -th weight parameters of decoder $\mathcal{D}^{(i)}$ by performing element-wise multiplication between $\mathcal{D}^{(i)}$ and the mapped message, where the i -th fully connected layer $\mathcal{F}\mathcal{C}^{(i)}(m') : \mathbb{R}^{d_{m'}} \rightarrow \mathbb{R}^{d_D^{(i)}}$ is applied to match the dimension, where $d_D^{(i)}$ is the input channel dimension of i -th weight parameters $\mathcal{D}^{(i)}$. Normalization is applied to ensure consistent scaling of the mapped message. The modulated weights in the i -th layer are defined as:

$$\mathcal{D}_{mod}^{(i)} = \mathcal{D}^{(i)} \circ \left(\frac{\mathcal{F}\mathcal{C}^{(i)}(\mathcal{M}(m)) - \mu^{(i)}}{\sigma^{(i)} + \epsilon} \cdot \gamma^{(i)} + \beta^{(i)} \right), \quad (1)$$

where $\gamma^{(i)}$ and $\beta^{(i)}$ are the i -th learnable parameters, while $\mu^{(i)}$ and $\sigma^{(i)}$ represent the mean and standard deviation of the message $\mathcal{F}\mathcal{C}^{(i)}(\mathcal{M}(m))$. In our experiments, we find that modulating every layer of the decoder \mathcal{D} leads to video quality degradation because it alters the parameters that have a significant impact on video generation. To minimize the undesirable impact on visual quality, we introduce importance-based weight modulation, which targets only the parameters with minimal effect on visual quality. To determine which layers to modulate, we first mea-

sure their importance. Specifically, before training, we sequentially add perturbations drawn from a normal distribution, $p \sim \mathcal{N}(0, 1)$, to each layer, resulting in the perturbed weights $\mathcal{D}_{perturbed}^{(i)} = \mathcal{D}^{(i)} + p$. By evaluating the LPIPS [52] metric, which measures perceptual similarity, on videos generated with sequentially perturbed layers, our method identifies which layers have a greater impact on video quality. It modulates the least important 50% of the layers, which have less impact on the video quality.

4.2. Distortion Layer

Robustness against various video attacks is essential yet remains challenging for existing watermarking methods [23, 25]. To address this, we apply random distortions to the generated video in every iteration before extracting the message. We employ two types of distortions: spatial distortions and compression distortions. Spatial distortions refer to pixel-level distortions within each frame, such as cropping and blurring, which can be easily integrated. However, adapting to compression distortions, particularly H.264 compression, poses challenges during training due to their non-differentiable nature. To address this issue, we design an H.264 network inspired by DVMark [23] and train it to accurately replicate real H.264 compression, enhancing the robustness against H.264 compression.

4.3. Robust Video Watermark Decoder

As seen in the bottom-right of figure 2, we design a watermark decoder \mathcal{W} that extracts messages by leveraging spatio-temporal information through the fusion of two domains: the generated RGB video \hat{v} and its 3D wavelet transformed subband \hat{v}_{freq} . We use only the low frequency subband LLL among the 3D wavelet subbands to enhance robustness against video compression, as various compression methods discard high-frequency features [19].

The watermark decoder is composed of two primary components: a feature extraction module and a feature fusion module. Before combining RGB domain and frequency domain, we first extract each domain’s features independently. Using six 3D convolutional blocks, we extract wavelet features $F_{freq} \in \mathbb{R}^{B \times 2048 \times F \times H \times W}$ from the low frequency subband LLL , where B , F , H , and W denote batch, frame, height, and width, respectively. On the other hand, we employ the ResNet50 model to extract spatial features $F_{rgb} \in \mathbb{R}^{B \times 2048 \times F \times H \times W}$ from the RGB video \hat{v} .

To efficiently fuse these two features, we employ temporal and spatial cross-attention mechanisms. The temporal cross-attention measures the attention score across frames, while the spatial cross-attention measures the attention score across height and width. The temporal and spatial cross-attention modules share the same architecture, each designed with 8 multi-heads. The entire feature fusion module consists of temporal cross-attention, spatial cross-

attention, and a position-wise feed-forward network, with a depth of 2. We set the wavelet features as the query $Q = \text{FC}_q(F_{freq})$, while using the spatial features as the key $K = \text{FC}_k(F_{rgb})$ and the value $V = \text{FC}_v(F_{rgb})$, where FC_q , FC_k and FC_v denote a fully connected layer for query, key, and value, respectively. This allows the spatial feature F_{rgb} to capture information from the wavelet features F_{freq} by leveraging the attention scores computed between them. The cross-attention module CA is defined as:

$$CA(F_{freq}, F_{rgb}) = \text{softmax}\left(\frac{Q \cdot K^T}{\sqrt{d_k}}\right) \cdot V. \quad (2)$$

The output of each cross-attention module is added to the spatial feature F_{rgb} for residual connection. With this watermark decoder, we obtain the message hidden within the generated video.

4.4. Training Objectives

We design our objective function to balance the trade-off between visual quality and watermark decoding accuracy. We employ binary cross-entropy loss between the random message m and the extracted message \hat{m} from the generated video to ensure accurate watermark decoding:

$$\begin{aligned} \mathcal{L}_{message} = & -\frac{1}{N} \sum_{i=1}^N m_i \cdot \log(\sigma(\hat{m}_i)) \\ & + (1 - m_i) \cdot \log(1 - \sigma(\hat{m}_i)), \end{aligned} \quad (3)$$

where N is the total number of message bits, while $\sigma(\cdot)$ denotes the sigmoid function. In addition, to enhance the visual quality of the generated video, we choose the Watson-VGG perceptual loss [10], which is designed to avoid blurring effects and visual artifacts of generated images:

$$\mathcal{L}_{lrips} = \text{VGG}(\mathcal{D}_{mod}(\mathcal{M}(m), \mathcal{E}(v)), v), \quad (4)$$

where \mathcal{D}_{mod} , \mathcal{M} , and \mathcal{E} denote the modulated latent decoder, mapping network, and latent encoder, respectively, while m and v are the random message and input video.

Furthermore, we propose a weighted patch loss to address localized artifacts in the generated video. We first compute the mean absolute error (MAE) for video patches, resulting in a loss score map normalized between 0 and 1 using the softmax function. By multiplying the patch MAE by the score map, we create a weighted patch loss that places more emphasis on areas with higher MAE, where artifacts are likely to occur. The weighted patch loss is as follows:

$$\mathcal{L}_{patch} = \frac{1}{P} \sum_{i=1}^P |\hat{v}_i - v_i| \cdot \text{softmax}(|\hat{v}_i - v_i|), \quad (5)$$

where P denotes the number of patches. The final objective can be formulated as:

$$\mathcal{L} = \lambda_{message} \mathcal{L}_{message} + \lambda_{lpips} \mathcal{L}_{lpips} + \lambda_{patch} \mathcal{L}_{patch}, \quad (6)$$

where $\lambda_{message}$, λ_{lpips} , and λ_{patch} are hyperparameters that balance three loss functions.

5. Experiments

5.1. Dataset

Video dataset. We train our method on Panda-70M dataset [7], a large-scale collection of video frames recognized for its diversity across various content types. We randomly download 10K videos from this dataset. Following the approach of Stable Video Diffusion [3], we sample 8 frames from each video, with each frame resized to a resolution of 256×256 for training.

Prompt dataset. We evaluate text-to-video generation on the Vidprom dataset [40], using prompts generated by GPT-4 [1]. To evaluate our method, we randomly sample 100 prompts from the dataset, which do not contain personally identifiable information or offensive content.

5.2. Implementation Details

Video diffusion models are generally categorized into two types: DiT [28] and U-Net [33] architectures. To evaluate our method on DiT architecture, we employ OpenSora [54], an open-source text-to-video-generative model. For the U-Net architecture, we utilize DynamiCrafter [44], which is the notable superior in video quality for text-image-to-video. We follow the same approach as DynamiCrafter by collecting images. Notably, these images are exclusively utilized in DynamiCrafter to generate videos for our evaluation process. For training, we only utilize the latent decoder of these models. Our method is trained on 10K videos (8 frames, 256×256 resolution) from Panda-70M dataset [7]. We modulate 50 % of the latent decoder layers to embed the message. For optimization, we set $\lambda_{message} = 0.8$, $\lambda_{lpips} = 0.7$, $\lambda_{patch} = 10$ in Eq. 6. Furthermore, we employ 100 random messages.

5.3. Evaluation

We evaluate three essential aspects of digital watermarking, which exhibit trade-offs: 1) *invisibility*, which is investigated by PSNR, SSIM, and LPIPS [52] to measure the video quality compared to the original. 2) *capacity*, investigated with 32-bit and 48-bit messages. 3) *robustness*, evaluated using Crop (retain 50 %), Rotation ($\pi/6$), Gaussian Blur (standard deviation = 1.0) and JPEG Compression (70 % of the original). We apply these attacks to each frame of the video. Since our task is video watermarking, we also consider video-specific distortions, such as Frame Swap (change 50 % positions of frames), Frame Average

(average of 6 frames), Frame Drop (Drop 50 % frames), and H.264 (crf=21), which is a widely used video compression technique. We also measure the robustness against a combination of Rotation, Frame Drop, and H.264 attacks. To evaluate the video quality, we report the tLP [9], which is used to measure the temporal consistency of the watermarked videos, and Fréchet Video Distance (FVD) [38], which is a metric for the temporal consistency of video generation.

Baseline. To the best of our knowledge, there is no watermarking method for the video diffusion models. Therefore, we compare with four strategies for a fair comparison: 1) **HiDDeN** [55], is the first deep learning image watermarking method. We embed the same message into each video frame. 2) **Blind** [25], is the traditional video watermarking method, using 3D Discrete Wavelet Transform. We follow the implementation in Blind [25]. 3) **Stable Signature** [12], is the watermarking method for the text-to-image diffusion model. 4) **WOUAF** [18], is the state-of-the-art watermarking method for the text-to-image diffusion model. For both Stable Signature and WOUAF, we train Open-Sora [54] and DynamiCrafter [44] using the same training set as our method. Additionally, we decode the message from each video frame for HiDDeN, Stable Signature, and WOUAF.

5.4. Experimental results

Video Quality and Bit Accuracy. There is a trade-off between video quality and bit accuracy, making it a key challenge in digital watermarking to improve both simultaneously. We first compare the generated video quality and bit accuracy of our method against other approaches, as shown in Figure 3 and Table 1. We observe that Stable Signature [12] and WOUAF [18] fail to generate high-quality videos with an invisible message when extended to video generation. HiDDeN [55] does not fully address temporal consistency, as it independently embeds the invisible message into each frame of the generated video. Though Blind [25] is a traditional video watermarking method, it fails to ensure temporal consistency on synthetic videos, as demonstrated by tLP and FVD evaluations, highlighting its limitations in handling generated videos. In contrast, as shown in Figure 3, and Table 1, our method preserves video quality, including temporal consistency, while achieving the highest bit accuracy. To illustrate the differences between the original and watermarked video, we present the normalized pixel intensity difference in Figure 4, following previous watermarking visualization methods [5, 13, 30]. Our method shows the smallest difference, demonstrating superior visual quality (more details in Section 5.5).

Video Quality and Capacity. In this section, we analyze video quality and bit accuracy based on the length of the embedded message. We compare our method with others

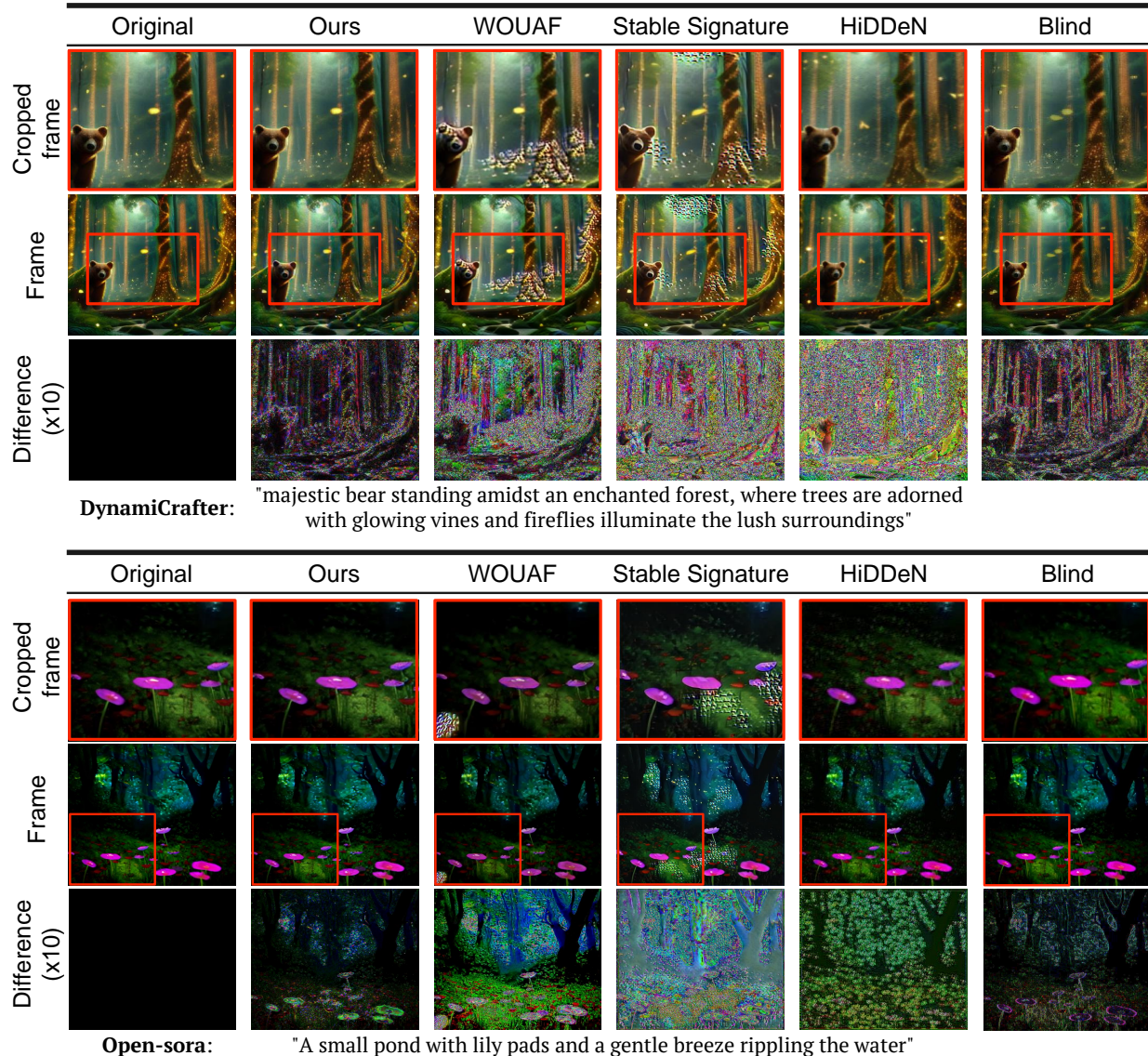


Figure 3. **Qualitative results with baselines.** We show the visual quality of generated videos with baseline watermarking methods. The first row shows the crop of each image, while the second and third rows show the video frame itself and the difference map ($\times 10$) between the original and each method.

Bit	Method	Open Sora						DynamyCrafter					
		Bits Acc.(%) \uparrow	PSNR \uparrow	SSIM \uparrow	LPIPS \downarrow	tLP \downarrow	FVD \downarrow	Bits Acc.(%) \uparrow	PSNR \uparrow	SSIM \uparrow	LPIPS \downarrow	tLP \downarrow	FVD \downarrow
32	HiDDeN [55]	90.83	30.20	0.901	0.265	5.493	2707.9	90.48	30.19	0.887	0.187	5.410	1637.7
	Blind [25]	92.05	28.88	0.888	0.251	5.615	1278.9	87.56	26.44	0.852	0.239	5.348	1390.2
	Stable Signature [12]	86.32	21.71	0.681	0.285	3.307	494.8	87.65	21.39	0.541	0.162	0.511	249.2
	WOUAF [18]	87.28	23.62	0.838	0.166	0.856	193.7	90.62	22.38	0.839	0.125	0.763	469.4
	Ours	94.44	31.15	0.919	0.105	0.219	65.73	96.00	31.50	0.892	0.075	0.173	85.49
48	HiDDeN [55]	85.62	29.85	0.888	0.269	6.802	2731.9	86.96	29.83	0.876	0.188	5.843	1716.5
	Blind [25]	87.41	27.79	0.872	0.204	4.845	1365.8	86.14	25.23	0.848	0.259	5.480	1480.1
	Stable Signature [12]	78.99	20.57	0.614	0.297	4.019	688.5	81.48	20.82	0.530	0.175	0.603	262.8
	WOUAF [18]	83.05	23.47	0.828	0.168	1.053	196.2	89.63	22.23	0.811	0.130	0.789	523.2
	Ours	90.42	30.32	0.910	0.117	0.287	117.5	93.67	30.78	0.889	0.100	0.240	155.0

Table 1. **Quantitative results.** We present the quantitative results for Open-Sora [54] and DynamyCrafter [44] with various watermarking methods: HiDDeN [55], Blind [25], Stable Signature [12], WOUAF [18] and LVMark, applied. The evaluation includes image metrics: PSNR, SSIM, LPIPS, video metrics: tLP [9], FVD [38], and bit accuracy on 32 and 48-bit messages.

		Bit Accuracy(%) \uparrow										Model Distortion (p=0.2)
		None	Crop (50%)	Rotation (+ $\pi/6$)	Gaussian Blur (std = 1.0)	JPEG Comp (70%)	Frame Swap (p=0.5)	Frame Avg. (n=6)	Frame Drop (p=0.5)	H.264 (crf=21)	Combine	
Open Sora	HiDDeN [55]	90.83	90.71	62.26	75.06	71.18	90.83	90.77	90.88	61.70	61.72	-
	Blind [25]	92.05	87.91	86.30	68.56	62.92	86.63	55.75	89.50	84.70	82.97	-
	Stable Signature [12]	86.32	78.42	54.26	84.15	76.65	86.32	77.43	76.72	81.31	51.82	77.58
	WOUAF [18]	87.28	79.79	78.62	86.94	85.66	87.28	81.91	82.19	81.24	76.21	75.33
	Ours	94.44	91.85	87.10	93.21	87.94	94.44	93.88	94.40	90.21	83.97	89.69
Dynamy Crafter	HiDDeN [55]	90.48	90.45	50.32	78.01	82.24	90.48	88.47	90.44	62.15	61.97	-
	Blind [25]	87.56	83.74	86.26	67.29	59.53	84.38	57.88	84.57	83.45	85.49	-
	Stable Signature [12]	87.65	84.15	50.39	82.20	77.44	87.65	83.97	85.97	83.94	51.62	80.98
	WOUAF [18]	90.62	90.59	89.03	88.41	87.99	90.62	88.61	90.50	89.70	88.42	78.36
	Ours	96.00	93.42	93.02	95.18	94.04	96.00	95.48	94.95	95.05	91.91	90.23

Table 2. **Robustness comparisons.** We present bit accuracy results of watermarking methods under various attacks, including image distortions, video distortions, combined distortions, and model distortions.

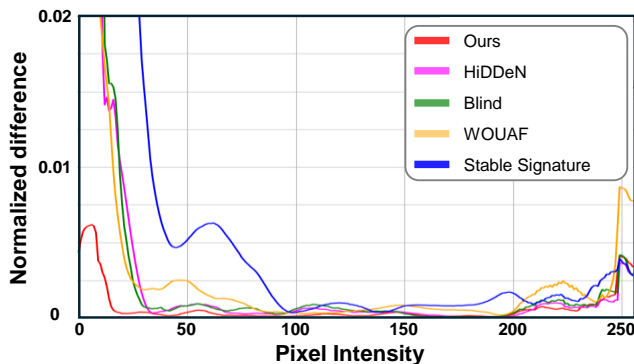


Figure 4. **Visualization of pixel intensity difference.** We show the normalized pixel intensity difference between original and watermarked videos. The red line depicts our results. A lower value on the y-axis indicates greater similarity to the original video.

for 32-bit and 48-bit messages, using 100 different messages. As shown in Table 1, all methods exhibit a decrease in bit accuracy as the message length increases. We note that our method achieves the highest bit accuracy compared to others, with over 90% bit accuracy at 48 bits. Furthermore, while all methods experience a noticeable drop in video quality as message length increases, our approach consistently shows a smaller decline across all metrics than other state-of-the-art methods. Our method also allows for embedding more messages in videos of comparable quality, outperforming others in both bit accuracy and video quality.

Robustness for Video Distortion. One of the priorities in digital watermarking is robustness against various distortions. In this section, we compare the robustness of our method with other approaches to demonstrate its effectiveness. As shown in Table 2, HiDDeN [55] is vulnerable to H.264 compression, while Blind [25] exhibits weaknesses against frame averaging, Gaussian blur, and JPEG compression. Additionally, Stable Signature [12] and WOUAF [18] fail to preserve the message when videos generated by the DiT model undergo rotation. In contrast, our method preserves the message across all attack metrics, thanks to the watermark decoder using 3D wavelet features.

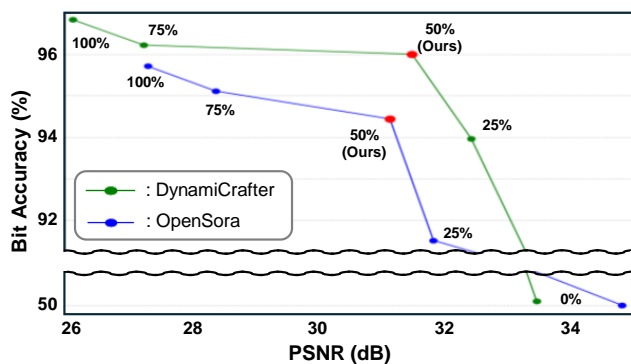


Figure 5. **The impact of weight modulation rate.** Each point represents the metrics obtained by training with a specific modulation rate. We experiment with modulation rates of 0%, 25%, 50%, 75%, and 100%.

Notably, it demonstrates exceptional robustness against video compression, especially H.264. We note that since all methods except Blind [25] are applied independently per-frame, it is naturally robust against frame drop.

Robustness for Model Distortion. We explore the scenario in which a malicious user, recognizing the existence of embedded messages in videos generated by the latent decoder, distorts the latent decoder to remove the embedded messages. We adopt a strategy that involves adding Gaussian noise ($\sigma = 0.05$) to the parameters of the latent decoder. We randomly select 20 % parameters of the latent decoder. Table 1 shows that our method ensures the presence of messages even when the latent decoder is distorted.

5.5. Ablation study

For the ablation study, we use the same configuration as described in Section 5.2, with 32-bit messages.

Weight modulation for watermarking As mentioned in Section 4.1, we selectively modulate the weights of the latent decoder to embed messages. The modulation rate is an important factor, as there exists trade-off. As shown in Figure 5, we generate videos with k ranging from 0 to 100. As

	DWT Type	Bits Acc. \uparrow	PSNR \uparrow	tLP \downarrow	FVD \downarrow
Open	2D DWT	92.01	30.92	0.450	122.9
Sora	3D DWT (Ours)	94.44	31.15	0.219	65.73
Dynami	2D DWT	91.71	28.73	0.383	158.3
Crafter	3D DWT (Ours)	96.00	31.50	0.173	85.49

Table 3. **Comparison of different DWT types.** We evaluate the metrics of 2D DWT and 3D DWT.

	Domain Type	PSNR \uparrow	Bit Accuracy(%) \uparrow	
			None	H264(crf21)
Open	RGB only	30.64	89.85	87.83
	High Freq only	31.91	50.45	50.33
	Low Freq only	33.30	50.13	50.12
	High Freq + RGB	28.97	88.72	86.14
	Low Freq + RGB (Ours)	31.15	94.44	90.21
Dynami	RGB only	28.62	91.82	88.10
	High Freq only	31.16	50.38	56.25
	Low Freq only	29.79	51.04	50.19
Crafter	High Freq + RGB	28.07	90.10	88.95
	Low Freq + RGB (Ours)	31.50	96.00	95.05

Table 4. **Comparison of different domain types.** We evaluate the metrics for each domain type.

k increases, bit accuracy improves while video quality declines, illustrating a trade-off. We find an optimal balance between bit accuracy and video quality when k is set to 50.

Watermark Decoder with 3D DWT. Temporal consistency is a crucial factor in video watermarking and generation tasks. To address this, we employ the 3D Wavelet Transform (3D DWT), which captures spatio-temporal information and converts videos into wavelet signals. Table 3 shows the comparison between 3D DWT and 2D Discrete Wavelet Transform (2D DWT), which utilizes only spatial information. As shown in Table 3, our watermark decoder utilizing 3D DWT achieves the best temporal consistency, bit accuracy, and video quality.

Watermark Decoder with Low Frequency. As mentioned in Section 4.3, we initially utilize only the low frequency subband (LLL) among the 3D wavelet subbands. While this achieves high PSNR values, relying solely on the frequency domain limits bit accuracy, as shown in Table 4. By combining RGB features with the low frequency subband (LLL), we significantly enhance bit accuracy without compromising PSNR. This approach is particularly robust for decoding messages, even in H.264 compressed videos.

Impact of Weighted Patch Loss on the video. As depicted in Section 4.4, artifacts appear in localized areas of the generated videos. To address this issue, we design a loss func-

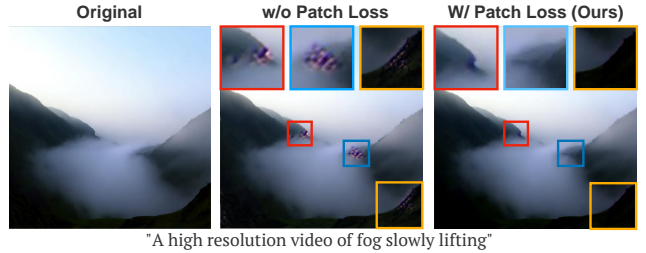


Figure 6. **Visual impact of weighted patch loss.** We visualize a video frame trained with and without weighted patch loss. To enhance clarity, we crop the local regions containing artifacts.

	Open Sora		DynamiCrafter	
	Bits Acc. \uparrow	LPIPS \downarrow	Bits Acc. \uparrow	LPIPS \downarrow
W/o Patch Loss	95.96	0.151	96.41	0.115
W/ Patch Loss (Ours)	94.44	0.105	96.00	0.075

Table 5. **Ablation on weighted patch loss.** We evaluate the impact of weighted patch loss.

tion that focuses on the regions where artifacts occur. Without the patch loss, although we achieve higher bit accuracy, the visual quality significantly degrades due to the presence of local artifacts, especially in the DiT model: Open-sora, which relatively focuses less on the local area by the nature of transformer architectures. Table 5 and Figure 6 demonstrate the effectiveness of the weighted patch loss in eliminating artifacts from local regions.

6. Conclusion

We proposed LVMark, a first watermarking method for video diffusion models.

Our method captures spatio-temporal information by effectively fusing the 3D wavelet domain and the RGB spatial domain for accurate message extraction from generated videos, even in the case of video modifications. Additionally, our method generates high-quality watermarked videos by selectively modulating latent decoder weights according to the importance of each layer. By balancing the trade-off between video quality and bit accuracy with tailored objective functions, including weighted patch loss, LVMark successfully embedded watermarks into video diffusion models. Experimental results showed that LVMark outperforms all the reasonable baseline methods.

Limitations. Our method demonstrates outstanding performance in the digital watermarking of video diffusion models. However, training the diffusion model to embed the watermark requires substantial memory due to the large size of the video diffusion models and the videos themselves, with memory usage reaching approximately 25GB. Future work could investigate memory-efficient watermarking methods for video diffusion models.

References

- [1] Josh Achiam, Steven Adler, Sandhini Agarwal, Lama Ahmad, Ilge Akkaya, Florencia Leoni Aleman, Diogo Almeida, Janko Altenschmidt, Sam Altman, Shyamal Anadkat, et al. Gpt-4 technical report. *arXiv preprint arXiv:2303.08774*, 2023. 5
- [2] Sadik AM Al-Taweel and Putra Sumari. Robust video watermarking based on 3d-dwt domain. In *TENCON 2009-2009 IEEE Region 10 Conference*, pages 1–6. IEEE, 2009. 2
- [3] Andreas Blattmann, Tim Dockhorn, Sumith Kulal, Daniel Mendelevitch, Maciej Kilian, Dominik Lorenz, Yam Levi, Zion English, Vikram Voleti, Adam Letts, et al. Stable video diffusion: Scaling latent video diffusion models to large datasets. *arXiv preprint arXiv:2311.15127*, 2023. 1, 2, 5
- [4] Andreas Blattmann, Robin Rombach, Huan Ling, Tim Dockhorn, Seung Wook Kim, Sanja Fidler, and Karsten Kreis. Align your latents: High-resolution video synthesis with latent diffusion models. In *Proceedings of the IEEE/CVF Conference on Computer Vision and Pattern Recognition*, pages 22563–22575, 2023. 2
- [5] Wang Cai-Yin, Kong Xiang-Wei, and Li Chao. Process color watermarking: the use of visual masking and dot gain correction. *Multimedia Tools and Applications*, 76:16291–16314, 2017. 5
- [6] Haoxin Chen, Yong Zhang, Xiaodong Cun, Menghan Xia, Xintao Wang, Chao Weng, and Ying Shan. Videocrafter2: Overcoming data limitations for high-quality video diffusion models. In *Proceedings of the IEEE/CVF Conference on Computer Vision and Pattern Recognition (CVPR)*, pages 7310–7320, 2024. 1, 2
- [7] Tsai-Shien Chen, Aliaksandr Siarohin, Willi Menapace, Ekaterina Deyneka, Hsiang-wei Chao, Byung Eun Jeon, Yuwei Fang, Hsin-Ying Lee, Jian Ren, Ming-Hsuan Yang, et al. Panda-70m: Captioning 70m videos with multiple cross-modality teachers. In *Proceedings of the IEEE/CVF Conference on Computer Vision and Pattern Recognition*, pages 13320–13331, 2024. 5
- [8] Ho Kei Cheng, Seoung Wug Oh, Brian Price, Joon-Young Lee, and Alexander Schwing. Putting the object back into video object segmentation. In *Proceedings of the IEEE/CVF Conference on Computer Vision and Pattern Recognition*, pages 3151–3161, 2024. 2
- [9] Mengyu Chu, You Xie, Jonas Mayer, Laura Leal-Taixé, and Nils Thuerey. Learning temporal coherence via self-supervision for gan-based video generation. *ACM Transactions on Graphics (TOG)*, 39(4):75–1, 2020. 5, 6
- [10] Steffen Czolbe, Oswin Krause, Ingemar Cox, and Christian Igel. A loss function for generative neural networks based on watson’s perceptual model. *Advances in Neural Information Processing Systems*, 33:2051–2061, 2020. 4
- [11] Fayaz Ali Dharejo, Muhammad Zawish, Yuanchun Zhou, Steven Davy, Kapal Dev, Sunder Ali Khowaja, Yanjie Fu, and Nawab Muhammad Faseeh Qureshi. Fuzzyact: A fuzzy-based framework for temporal activity recognition in iot applications using rnn and 3d-dwt. *IEEE Transactions on Fuzzy Systems*, 30(11):4578–4592, 2022. 2
- [12] Pierre Fernandez, Guillaume Couairon, Hervé Jégou, Matthijs Douze, and Teddy Furon. The stable signature: Rooting watermarks in latent diffusion models. In *Proceedings of the IEEE/CVF International Conference on Computer Vision*, pages 22466–22477, 2023. 1, 3, 5, 6, 7
- [13] Junhui He, Jiwu Huang, and Guoping Qiu. A new approach to estimating hidden message length in stochastic modulation steganography. In *International Workshop on Digital Watermarking*, pages 1–14. Springer, 2005. 5
- [14] Jonathan Ho, Tim Salimans, Alexey Gritsenko, William Chan, Mohammad Norouzi, and David J Fleet. Video diffusion models. *Advances in Neural Information Processing Systems*, 35:8633–8646, 2022. 2
- [15] Andrew Jaegle, Sebastian Borgeaud, Jean-Baptiste Alayrac, Carl Doersch, Catalin Ionescu, David Ding, Skanda Koppula, Daniel Zoran, Andrew Brock, Evan Shelhamer, et al. Perceiver io: A general architecture for structured inputs & outputs. *arXiv preprint arXiv:2107.14795*, 2021. 2
- [16] Andrew Jaegle, Felix Gimeno, Andy Brock, Oriol Vinyals, Andrew Zisserman, and Joao Carreira. Perceiver: General perception with iterative attention. In *International conference on machine learning*, pages 4651–4664. PMLR, 2021. 2
- [17] Milad Jafari Barani, Peyman Ayubi, Milad Yousefi Valandar, and Behzad Yosefnezhad Irani. A blind video watermarking algorithm robust to lossy video compression attacks based on generalized newton complex map and contourlet transform. *Multimedia Tools and Applications*, 79(3):2127–2159, 2020. 2
- [18] Changhoon Kim, Kyle Min, Maitreya Patel, Sheng Cheng, and Yezhou Yang. Wouaf: Weight modulation for user attribution and fingerprinting in text-to-image diffusion models. In *Proceedings of the IEEE/CVF Conference on Computer Vision and Pattern Recognition*, pages 8974–8983, 2024. 1, 5, 6, 7
- [19] Jong-Seok Lee and Touradj Ebrahimi. Perceptual video compression: A survey. *IEEE Journal of selected topics in signal processing*, 6(6):684–697, 2012. 4
- [20] Seunghoon Lee, Suhwan Cho, Dogyoon Lee, Minhyeok Lee, and Sangyoun Lee. Tsanet: Temporal and scale alignment for unsupervised video object segmentation. In *2023 IEEE International Conference on Image Processing (ICIP)*, pages 1535–1539. IEEE, 2023. 2
- [21] Xuefang Li and Rangding Wang. A video watermarking scheme based on 3d-dwt and neural network. In *Ninth IEEE International Symposium on Multimedia Workshops (ISMW 2007)*, pages 110–115. IEEE, 2007. 2
- [22] Hongmei Liu, Nuo Chen, Jiwu Huang, Xialing Huang, and Yun Q Shi. A robust dwt-based video watermarking algorithm. In *2002 IEEE International Symposium on Circuits and Systems (ISCAS)*, pages III–III. IEEE, 2002. 2
- [23] Xiyang Luo, Yinxiao Li, Huiwen Chang, Ce Liu, Peyman Milanfar, and Feng Yang. Dvmark: a deep multiscale framework for video watermarking. *IEEE Transactions on Image Processing*, 2023. 1, 2, 4
- [24] Xin Ma, Yaohui Wang, Gengyun Jia, Xinyuan Chen, Ziwei Liu, Yuan-Fang Li, Cunjian Chen, and Yu Qiao. Scaleable

- latent diffusion transformer for video generation. *arXiv preprint arXiv:2401.03048*, 2024. 1, 2
- [25] Majid Masoumi and Shervin Amiri. A blind scene-based watermarking for video copyright protection. *AEU-International Journal of Electronics and Communications*, 67(6):528–535, 2013. 4, 5, 6, 7
- [26] Nagita Mehrseresht and David Taubman. An efficient content-adaptive motion-compensated 3-d dwt with enhanced spatial and temporal scalability. *IEEE Transactions on Image processing*, 15(6):1397–1412, 2006. 2
- [27] Alexander Quinn Nichol and Prafulla Dhariwal. Improved denoising diffusion probabilistic models. In *International conference on machine learning*, pages 8162–8171. PMLR, 2021. 2
- [28] William Peebles and Saining Xie. Scalable diffusion models with transformers. In *Proceedings of the IEEE/CVF International Conference on Computer Vision*, pages 4195–4205, 2023. 2, 3, 5
- [29] Aditya Ramesh, Prafulla Dhariwal, Alex Nichol, Casey Chu, and Mark Chen. Hierarchical text-conditional image generation with clip latents. *arXiv preprint arXiv:2204.06125*, 1(2):3, 2022. 1
- [30] Alastair Reed, Tomáš Filler, Kristyn Falkenstern, and Yang Bai. Watermarking spot colors in packaging. In *Media Watermarking, Security, and Forensics 2015*, pages 46–58. SPIE, 2015. 5
- [31] Ahmad Rezaei, Mohammad Akbari, Saeed Ranjbar Alvar, Arezou Fatemi, and Yong Zhang. Lawa: Using latent space for in-generation image watermarking. *arXiv preprint arXiv:2408.05868*, 2024. 3
- [32] Robin Rombach, Andreas Blattmann, Dominik Lorenz, Patrick Esser, and Björn Ommer. High-resolution image synthesis with latent diffusion models. In *Proceedings of the IEEE/CVF Conference on Computer Vision and Pattern Recognition (CVPR)*, pages 10684–10695, 2022. 1
- [33] Olaf Ronneberger, Philipp Fischer, and Thomas Brox. U-net: Convolutional networks for biomedical image segmentation. In *Medical image computing and computer-assisted intervention—MICCAI 2015: 18th international conference, Munich, Germany, October 5–9, 2015, proceedings, part III 18*, pages 234–241. Springer, 2015. 3, 5
- [34] Chitwan Saharia, William Chan, Huiwen Chang, Chris Lee, Jonathan Ho, Tim Salimans, David Fleet, and Mohammad Norouzi. Palette: Image-to-image diffusion models. In *ACM SIGGRAPH 2022 conference proceedings*, pages 1–10, 2022. 1, 2
- [35] Mohammad Nazmus Sakib, Shuvashis Das Gupta, and Satyendra N Biswas. A robust dwt-based compressed domain video watermarking technique. *International Journal of Image and Graphics*, 20(01):2050004, 2020. 2
- [36] Jascha Sohl-Dickstein, Eric Weiss, Niru Maheswaranathan, and Surya Ganguli. Deep unsupervised learning using nonequilibrium thermodynamics. In *International conference on machine learning*, pages 2256–2265. PMLR, 2015. 2
- [37] Jaewon Son, Jaehun Park, and Kwangsu Kim. Csta: Cnn-based spatiotemporal attention for video summarization. In *Proceedings of the IEEE/CVF Conference on Computer Vision and Pattern Recognition*, pages 18847–18856, 2024. 2
- [38] Thomas Unterthiner, Sjoerd van Steenkiste, Karol Kurach, Raphaël Marinier, Marcin Michalski, and Sylvain Gelly. Fvd: A new metric for video generation. 2019. 5, 6
- [39] Ce Wang, Chao Zhang, and Pengwei Hao. A blind video watermark detection method based on 3d-dwt transform. In *2010 IEEE International Conference on Image Processing*, pages 3693–3696. IEEE, 2010. 1
- [40] Wenhao Wang and Yi Yang. Vidprom: A million-scale real prompt-gallery dataset for text-to-video diffusion models. *Thirty-eighth Conference on Neural Information Processing Systems*, 2024. 5
- [41] Yuxin Wen, John Kirchenbauer, Jonas Geiping, and Tom Goldstein. Tree-rings watermarks: Invisible fingerprints for diffusion images. In *Thirty-seventh Conference on Neural Information Processing Systems*, 2023. 1, 3
- [42] Yuxin Wen, John Kirchenbauer, Jonas Geiping, and Tom Goldstein. Tree-rings watermarks: Invisible fingerprints for diffusion images. *Advances in Neural Information Processing Systems*, 36, 2024. 1, 2
- [43] Fei Xie, Lei Chu, Jiahao Li, Yan Lu, and Chao Ma. Videotrack: Learning to track objects via video transformer. In *Proceedings of the IEEE/CVF conference on computer vision and pattern recognition*, pages 22826–22835, 2023. 2
- [44] Jinbo Xing, Menghan Xia, Yong Zhang, Haoxin Chen, Wangbo Yu, Hanyuan Liu, Gongye Liu, Xintao Wang, Ying Shan, and Tien-Tsin Wong. Dynamicrafter: Animating open-domain images with video diffusion priors. In *European Conference on Computer Vision*, pages 399–417. Springer, 2025. 1, 2, 5, 6
- [45] Zijin Yang, Kai Zeng, Kejiang Chen, Han Fang, Weiming Zhang, and Nenghai Yu. Gaussian shading: Provable performance-lossless image watermarking for diffusion models. In *Proceedings of the IEEE/CVF Conference on Computer Vision and Pattern Recognition*, pages 12162–12171, 2024. 2
- [46] Tianwei Yin, Michaël Gharbi, Richard Zhang, Eli Shechtman, Fredo Durand, William T Freeman, and Taesung Park. One-step diffusion with distribution matching distillation. In *Proceedings of the IEEE/CVF Conference on Computer Vision and Pattern Recognition*, pages 6613–6623, 2024. 2
- [47] Sahar Yousefi, MT Manzuri Shalmani, Jeremy Lin, and Marius Staring. A novel motion detection method using 3d discrete wavelet transform. *IEEE Transactions on Circuits and Systems for Video Technology*, 29(12):3487–3500, 2018. 2
- [48] Ning Yu, Vladislav Skripniuk, Dingfan Chen, Larry S. Davis, and Mario Fritz. Responsible disclosure of generative models using scalable fingerprinting. In *International Conference on Learning Representations*, 2022. 2, 3
- [49] Shigong Yu, M Omair Ahmad, and MNS Swamy. Video denoising using motion compensated 3-d wavelet transform with integrated recursive temporal filtering. *IEEE Transactions on Circuits and Systems for Video Technology*, 20(6):780–791, 2010. 2
- [50] Sihyun Yu, Kihyuk Sohn, Subin Kim, and Jinwoo Shin. Video probabilistic diffusion models in projected latent

- space. In *Proceedings of the IEEE/CVF conference on computer vision and pattern recognition*, pages 18456–18466, 2023. [2](#)
- [51] Qiang Zhang, Sheng Hua, Rick S Blum, and Minli Chen. Video fusion performance assessment based on spatial-temporal phase congruency. *Signal processing*, 105:43–55, 2014. [2](#)
- [52] Richard Zhang, Phillip Isola, Alexei A Efros, Eli Shechtman, and Oliver Wang. The unreasonable effectiveness of deep features as a perceptual metric. In *Proceedings of the IEEE conference on computer vision and pattern recognition*, pages 586–595, 2018. [1](#), [4](#), [5](#)
- [53] Xuanyu Zhang, Runyi Li, Jiwen Yu, Youmin Xu, Weiqi Li, and Jian Zhang. Editguard: Versatile image watermarking for tamper localization and copyright protection. In *Proceedings of the IEEE/CVF Conference on Computer Vision and Pattern Recognition*, pages 11964–11974, 2024. [2](#)
- [54] Zangwei Zheng, Xiangyu Peng, Tianji Yang, Chenhui Shen, Shenggui Li, Hongxin Liu, Yukun Zhou, Tianyi Li, and Yang You. Open-sora: Democratizing efficient video production for all, 2024. [1](#), [2](#), [5](#), [6](#)
- [55] Jiren Zhu, Russell Kaplan, Justin Johnson, and Li Fei-Fei. Hidden: Hiding data with deep networks. In *Proceedings of the European Conference on Computer Vision (ECCV)*, pages 1–17, 2018. [5](#), [6](#), [7](#)